16th World Conference on Earthquake Engineering, 16WCEE 2017
Santiago Chile, January 9th to 13th 2017
Paper N° 5002(Abstract ID)
Registration Code: S-U1478038471

GEER-ATC M_w7.8 ECUADOR 4/16/16 EARTHQUAKE RECONNAISSANCE PART II: SELECTED GEOTECHNICAL OBSERVATIONS

X. Vera-Grunauer[1], S. Nikolaou[2], R. Gilsanz[3], G. Diaz-Fanas[4], N. Antonaki[5], S. Lopez[6], R. Luque[7], B. Casares[8], A. Caicedo[9], D. Alzamora[10], K. Rollins[11], C. Wood[12], A. Athanasopoulos-Zekkos[13], G. Lyvers[14], V. Diaz[15], T. Toulkeridis[16], E. Morales[17]

[1] *Head of the Engineering Research Institute, Instituto de Ingeniería, Universidad Católica Santiago de Guayaquil, Geoestudios, Ecuador, xvg@geoestudios.com.ec*
[2] *Principal, Multi-Hazards & Geotechnical Engineering, WSP|Parsons Brinckerhoff, nikolaous@pbworld.com*
[3] *Founding Partner, Structural Engineer, Gilsanz Murray Steficek LLP, USA, ramon.gilsanz@gmsllp.com*
[4] *Geotechnical Engineer, WSP|Parsons Brinckerhoff, diazfanasg@pbworld.com*
[5] *Geotechnical Engineer, WSP|Parsons Brinckerhoff, antonakin@pbworld.com*
[6] *Geotechnical Engineer, Geoestudios, Ecuador, slopez@geoestudios.com.ec*
[7] *PhD Candidate, University of California, Berkeley, obluque@gmail.com*
[8] *Undergraduate Student, Cornell University, USA, bc473@cornell.edu*
[9] *Geotechnical Engineer Researcher, Universidad Católica de Santiago de Guayaquil, Ecuador (UCSG), acaicedoaspiazu@gmail.com*
[10] *Geotechnical Engineer, Federal Highway Administration, USA, daniel.alzamora@dot.gov*
[11] *Professor, Brigham Young University, USA, rollinsk@byu.edu*
[12] *Assistant Professor, Univ. of Arkansas, USA, cmwood@uark.edu*
[13] *Associate Professor, UMICHIGAN, USA, addazekk@umich.edu*
[14] *Structural Engineer, Army Corp of Engineers, USA, gabriela.m.lyvers@usace.army.mil*
[15] *Senior Structural Engineer, Gilsanz Murray Steficek LLP, USA, virginia.diaz@gmsllp.com*
[16] *Professor and Researcher of Geology, Geochemistry, Volcanology, Escuela Politecnica del Ejercito, EC, theofilost@usfq.edu.ec*
[17] *PhD Candidate, Univ. at Buffalo & L. Colonel of EC Army Corps of Engineers, enriquea@buffalo.edu*

Abstract

On the evening of April 16th, 2016, a moment magnitude M_w7.8 earthquake struck northern Ecuador, offshore of its west coast. The earthquake was named Muisne after the city of its epicenter, located about 29 km south-southeast of the town of Muisne, in the province of Manabí, at a hypocentral depth of 21 km. In the first 24 hours, over 135 aftershocks were recorded with hundreds more in the weeks that followed. Overall, this earthquake and its aftershocks led to hundreds of fatalities, thousands of injuries, tens of thousands homeless and an economic impact estimated at 3% of the nation's Gross Domestic Product (GDP). This paper is the second part of two papers that will present selected geotechnical reconnaissance observations from this earthquake, including site conditions, earthquake-induced damage, soil amplification and liquefaction, based on the reconnaissance findings from the mission of the team deployed by the Geotechnical Extreme Event Reconnaissance (GEER) Association and the Applied Technology Council (ATC) with a detailed report available at www.geerassociation.org.

Keywords: earthquake reconnaissance; geotechnical observations; liquefaction; site amplification; ports; GEER; ATC.

1. Introduction

The main M_w7.8 earthquake hit Ecuador on April 16th, 2016, centered offshore of the west coast of northern Ecuador, followed by many aftershocks. Based on the United States Geological Survey (USGS), the main event was caused by shallow thrust faulting on or near the plate boundary between the Nazca and South America plates, where the Nazca subducts beneath the South America plate at a rate of 61 mm/yr. Subduction along the Ecuador and the Peru-Chile trenches farther south has led to uplift of the Andes mountains and has produced some of the largest known earthquakes, including the largest ever recorded M9.5 Chile earthquake in 1960.

The event drew the attention of the Geotechnical Extreme Events Reconnaissance (GEER) Association, due to the several hundred casualties, tens of thousands homeless, and destruction along the west coast, with evidence of severe ground shaking and geotechnical failures. GEER had activated a reconnaissance team with funding by the National Science Foundation (NSF) when a second major M_w6.1 event occurred on April 20th. The GEER team was joined by structural engineers funded by the Applied Technology Council (ATC). The US-based team was on the ground from April 26th to May 2nd, joined by Ecuadorian counterpart partners.

The GEER-Ecuador team was co-led by Dr. Sissy Nikolaou of WSP | Parsons Brinckerhoff (WSP|PB) from the US and Dr. Xavier Vera-Grunauer of the Universidad Católica de Santiago de Guayaquil and of the Geoestudios firm of Ecuador (EC). The NSF-funded GEER members that travelled to Ecuador were geotechnical engineers Mr. Daniel Alzamora (Federal Highway Administration), Prof. Adda Athanasopoulos-Zekkos (Univ. of Michigan), Ms. Gabriela Martinez Lyvers (US Army Corp of Engineers), Prof. Kyle Rollins (Brigham Young Univ.), and Prof. Clint Wood (Univ. of Arkansas). The US team members funded by ATC were structural engineers Mr. Ramon Gilsanz of Gilsanz Murray Steficek (GMS) and Ms. Virginia Diaz (GMS), who was the ATC recorder for the report preparation.

The GEER-ATC group joined other US team members, already in Ecuador, funded individually or by their institutions, including Prof. Eduardo Miranda (Stanford Univ.), Mr. Enrique Morales (Univ. at Buffalo; Lt. Colonel of EC Army Corps of Engineers), and Mr. Roberto Luque (Univ. of California at Berkeley). During the reconnaissance, Mr. Guillermo Diaz-Fanas (WSP|PB) served as GEER-Ecuador recorder for the information gathered and the US contact person along with Mr. Pablo Lopez (PE) who facilitated communications while aboard. The GEER-ATC USA team was joined by Ecuadorian partners from the government, army, universities, and private engineering firms and by a Colombian partner from Universidad Norte, Prof. Carlos Arteta. The Ecuador-USA GEER-ATC team met daily to discuss findings and plan the following days.

This paper is the second of two papers in this conference that will present selected geotechnical aspects including site conditions, earthquake-induced damage, soil amplification and liquefaction, from the main Mw7.8 Muisne, Ecuador earthquake. More details can be found in [1] and [2].

2. Site Effects

The background on the unique seismotectonic setting of Ecuador and its historic seismicity, along with the strong motion recordings from the Mw7.8 April 16th, 2016 earthquake have been presented in Part 1 of this paper. This recent event has confirmed that the regional subsurface conditions can generate significant amplification of the seismic waves propagating from the bedrock, or liquefy or loose strength under strong shaking. This section will present site conditions and associated soil amplification effects at two densely populated cities, Guayaquil and Portoviejo, located 170 and 73 km from the epicenter, respectively.

2.1 Portoviejo

Portoviejo was one of the hardest hit areas in the April earthquake. The city is situated on an alluvial plain between colluvial deposits (green area of Figure 1). Two characteristic soil profiles are presented on Figure 1: APO1 (at the location of the IGN strong motion station) and Los Tamarindos. APO1 is located in the transition

between alluvial soils and coluvial deposits with an average shear wave velocity at the top 30 m, V_{s30} of 240 m/s, while Los Tamarindos is in the middle of the alluvial clay and silt deposits with, V_{s30} of 220m/s. The V_s profiles shown next to the stratigraphy on the same figure have been derived from geotechnical subsurface investigations that either included in-situ geophysical testing or correlated Standard Penetrometer Test (SPT) N-values to low-strain shear modulus G and V_s. The elastic site period, T_e, at APO1 was estimate to be 0.38 s and at Los Tamarindos 0.50 s, with expected differences due to the depths to the siltstone rock.

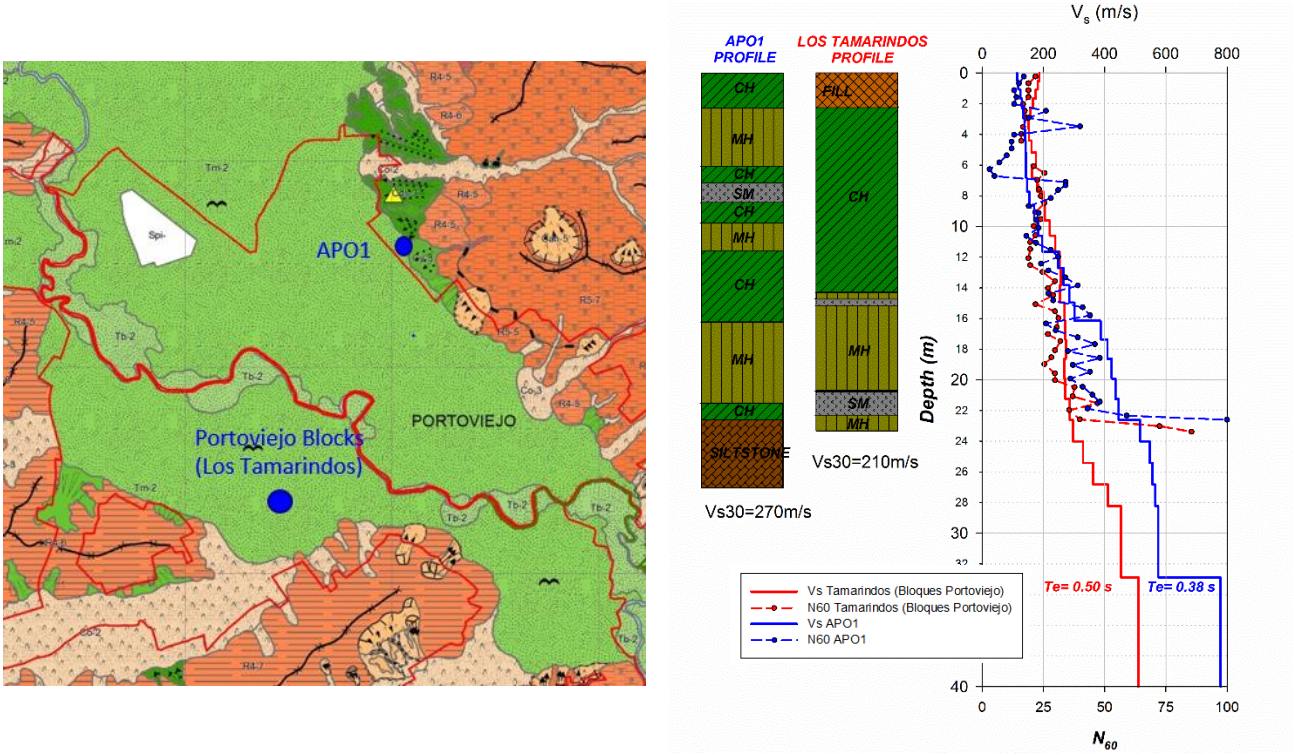

Figure 1. Portoviejo city: Geologic map (left); typical stratigraphy at APO1 station and Los Tamaridos sites (middle); and estimated shear wave velocity profiles for these sites (right) (modified from [1])

The damage caused by the earthquake was mainly concentrated in the downtown area, where most of the buildings are taller than 4 stories. The distribution of damage as function of building height is presented on Figure 2 that demonstrates that damage increases with building height and the estimated structural period. The buildings are founded on different zones of the alluvial clayey deposits, so their response is likely affected by the site conditions. At Station APO1, large soil amplification is evident as shown on Figure 2 with peak Spectral acceleration Sa ~ 2g and ratio of Sa/PGA from 4.5 to 5.5 in the period range of 0.4 to 0.5 s, with an elastic site period of 0.38 s. The inelastic induced site period (Ts) for Station APO1 is about 0.5s and the Ts/Te relation is 1.3. Based on deconvolution analysis it was found a localized induced maximum shear strain at 7 meters depth of 1.2%.

Figure 3 presents photos of a 6-story reinforced concrete building before and after the earthquake that caused it to collapse, with an estimated fundamental structural period between 0.58 to 0.7 s. At the same figure, the 2-story wood house suffered only slight damage with an estimated fundamental structural period between 0.1 to 0.2 s.

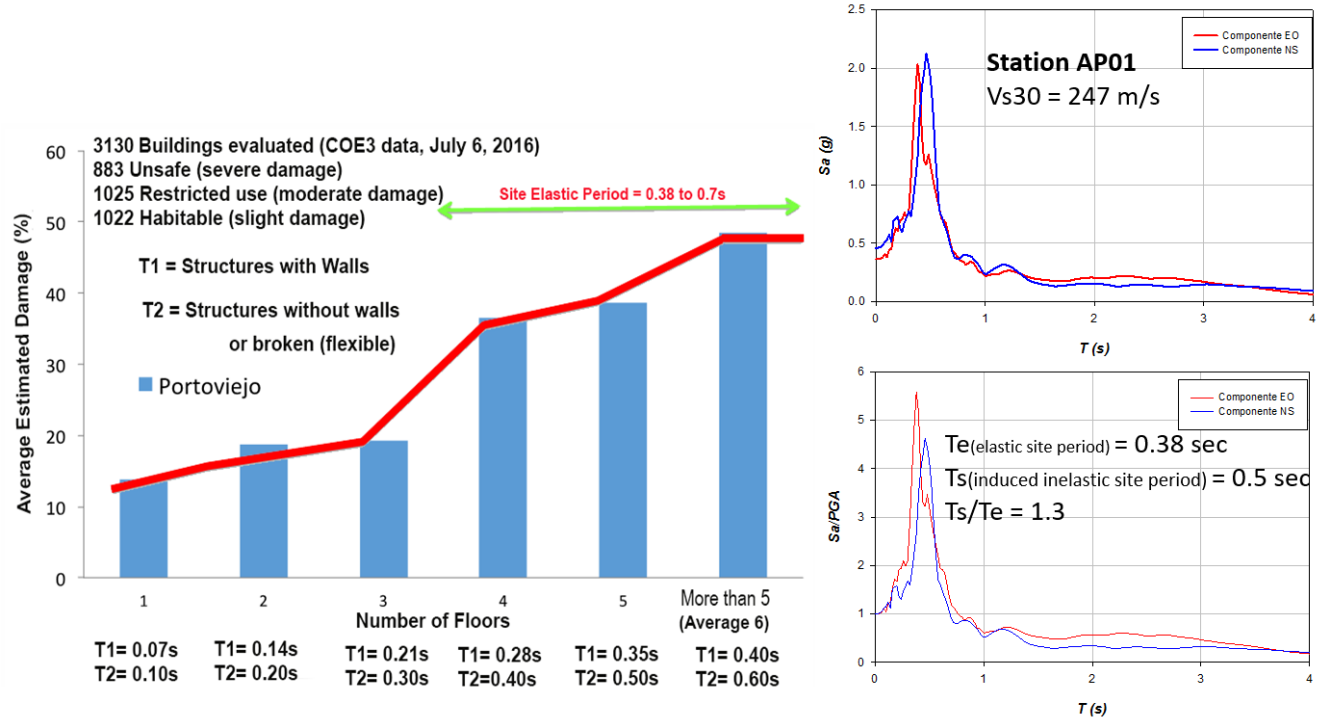

Figure 2. (a) Average estimated damage in Portoviejo based on ATC procedures and (b) acceleration response spectra for 5% structural damping for station APO1 with its normalized acceleration response spectra (modified from [1]).

Figure 3. Portoviejo photos of buildings before (left) and after the earthquake (right). The 6-story reinforced building collapsed and the 2-story wood building survived (modified from [1]).

3.2 Guayaquil

The city of Guayaquil is a major seaport on the left bank of the Guayas River and the largest urban area of Ecuador, with a population of more than 2.3 million. As many cities located at the edge of a navigable river, the underlying soils at Guayaquil were deposited under water. Hence, they are generally soft and compressible. Cretaceous hard sedimentary rock (Cayo formation) underlies the deep soft sediments[3]. The ground is mostly in low elevations with groundwater close to the surface, which often requires compaction of the upper fills before construction. The map of **Figure** 4 [4] shows the geotechnical zones and strong motion stations of Guayaquil.

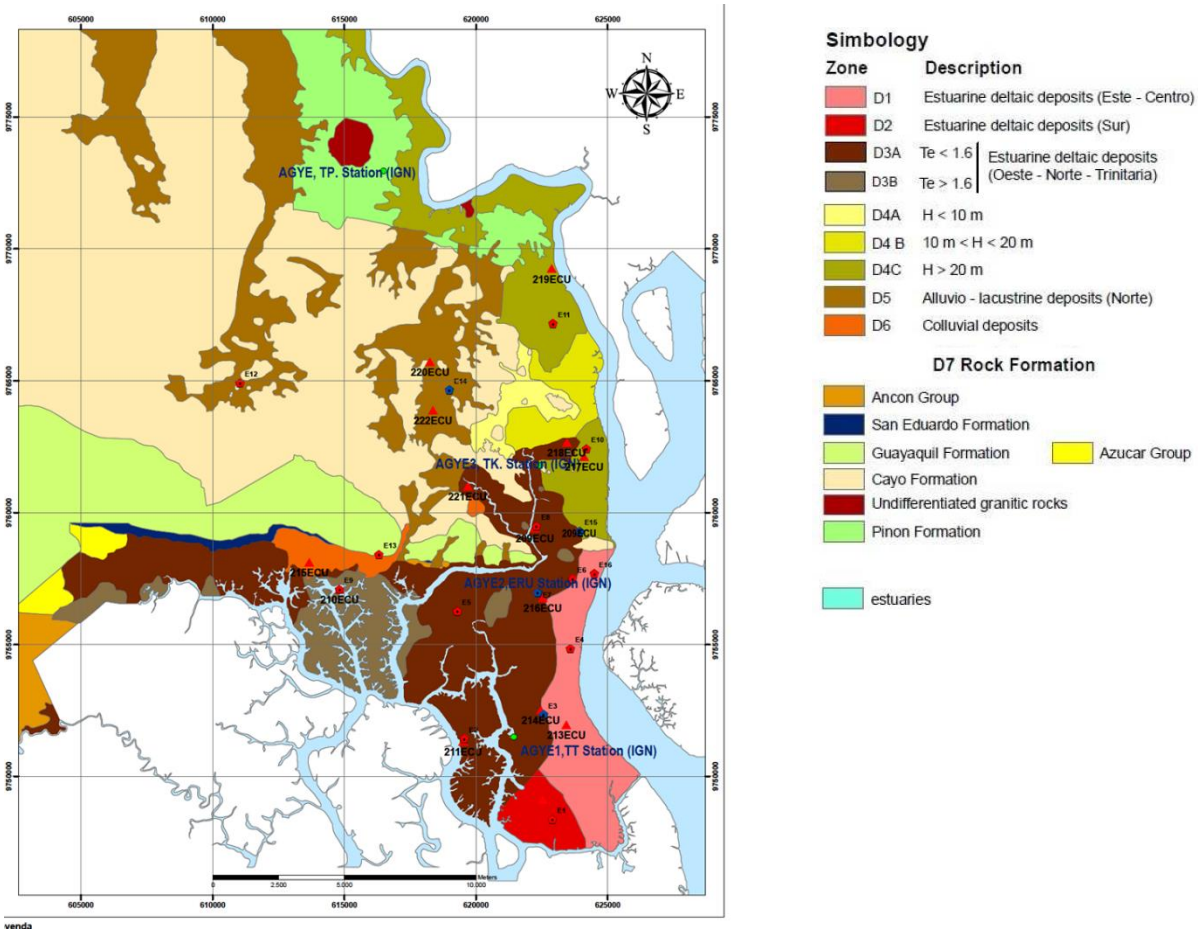

Figure 4. Geotechnical Zones of Guayaquil and the location of the IGN ground motion stations [3].

Guayaquil is mostly built over estuarine-deltaic and alluvial deposits, with only small portion in the north and northwest area built on shallow lacustrine and colluvium/residual deposits. Zones D1, D2 and D3 located at the south and west of the city consist of deep soft clayey soils with pyrite cementation and diatoms[5]. These soils are classified as Type F according to the Ecuadorian Construction Standards 2015 (NEC-2015)[6]. Zone D4 is in an alluvial valley at the north and has similar composition to zones D1 through D3, but without pyrite cementation and diatoms, and with deeper bedrock. This site is classified as Type E according to the NEC-15[6]. Zone D5 is at the northwest, composed of alluvial lacustrine deposits (shallow high plasticity clay overlaying sedimentary rock) and is classified as Type F because it has a high impedance contrast within 30-m depth. Zone D6 with colluvium soils are classified as Type C. Zone D6 is alluvial at the west, and D7 consists of residual soil deposits and outcropping rock, classified as Type A or Type B according to the NEC-15 [6].

The three strong ground motion stations of Guayaquil are shown on Figure 4: AGYE2 ERU is located in downtown; AGYE and TP in Pascuales at the north, and UCSG of the Catholic University of Guayaquil is at the west. AGYE2 is within zone D3, while AGYE, TP and UCSG stations are within Zone D7, in outcropping igneous rock from Piñon formation and sedimentary rocks from Cayo formation, respectively. Shear wave velocity (V_s) profiles have been estimated for each of the stations derived from data collected from the two subsurface investigations, either directly with geophysical testing, or with correlations of low-strain V_s or shear modulus G with the SPT and Cone Penetrometer Testing (CPT) results.

Based moderate-intensity ground motions recorded in 2012, the elastic site period estimated for AGYE2 using the V_s estimate for this site is 1.5 s, a high value typical of soft clayey soils. Using the elastic period map

of Guayaquil City from the Nakamura method the anticipated site period at this site range from 1.4 to 1.6 s[4]). V_{s30} estimates for AGYE TP and UCSG stations are 1,822 and 1,200 m/s, respectively which classifies AGYE TP as Type A and UCSG as Type B according to the NEC-15[6].

Extensive geotechnical investigations and laboratory tests have been performed to determine the static and dynamic soil properties of the deltaic estuarine greenish gray GYE-CLAY (in Zone D3), including falling cone test (FCT), laboratory vane test (LVT), constant rate consolidation test (CRS), direct simple shear test (DSS), triaxial undrained compresion anisotropicaly consolidated (CKUC), cyclic simple shear test (CSS), and cyclic triaxial isotropically consolidated undrained test (CUIC)[5]. In addition, the Simsoil constitutive model[7] was calibrated to capture the confining stress effect in the modulus reduction and damping curves. As a result of micro-structure analyses (fabric, composition and inter-particle forces) of the GYE-CLAY, a unique behavior within the zone D3 was discovered: this material is composed of cemented clays with pirite and diatoms. The cementation reduces the damping with respect to "conventional soil" with similar index properties and can increase the site amplification[5].

Figure 5 presents the PGA amplification between the soil and rock (PGA_{soil}/PGA_{rock}) for the Cayo formation. Low intensity earthquakes of 2012 and 2015 are included, together with estimations for the deltaic estuarine deposits for high intensity earthquakes. The April 16th main earthquake records in the two components fits well with the average calculated from nonlinear total stress analyses in the different geotechnical zones of Guayaquil. Amplification (PGA soil at AGYE2 station and the estimated PGA rock at UCSG station) of 3.5 and 2.7 were observed for NS and EW component, respectively.

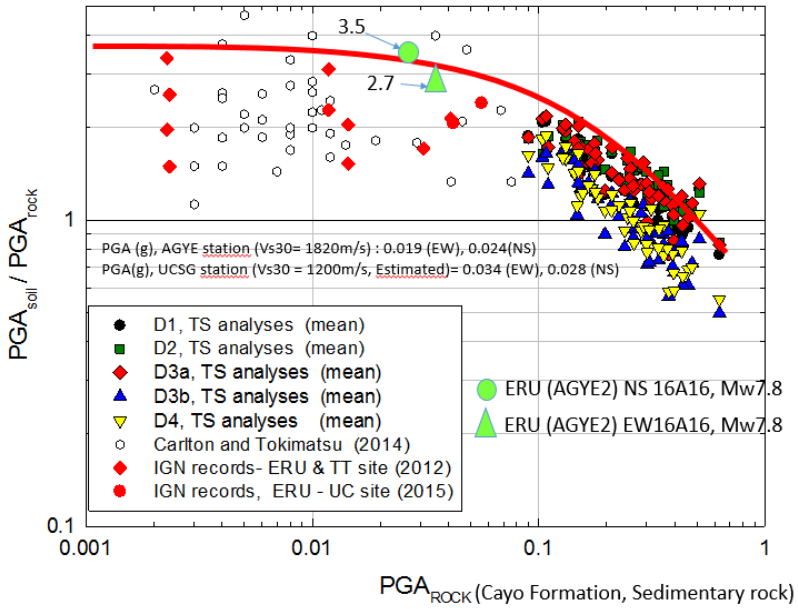

Figure 5. Guayaquil: Peak Ground Accelerations (PGA) relation between soil and rock for the PGA of Cayo Formation, modified from Vera-Grunauer (2014)[4]

The station AGYE TP is located in Type A and the UCSG stations in Type B site conditions. AGYE TP station is located in outcropping igneous rock from Piñon formation, while UCSG station is located at the sedimentary rocks from Cayo formation. Seismic records were obtained for the April 2016 earthquake for all the stations; however, for the UCSG record only partial information was recorded. In order to perform valid comparisons between stations response, the time histories of AGYE2 and AGYE TP stations had to be adjusted to the measured time of the UCSG partial time-history record.

Using the adjusted seismic record of Pascuales (AGYE, TP), scaling factors were estimated based on Fourier amplitude spectra ratio between the UCSG (Cayo formation) and AGYE TP (Piñon formation) stations as shown on Figure 6. The period range of 0.7 to 4 s (1.4 to 0.25 Hz) was considered to obtain the scaling factors

which will define the transfer functions (from AGYE TP to UCSG station) for the input motion at outcropping rock in AGYE2 soil column. Scaling factors of 1.8 and 1.2 were obtained for the EW and NS components, respectively. The scaled input seismic records were considered to be characteristic for outcropping motion for Cayo formation (Type B). Then, wave propagation analyses using the software DMOD and SHAKE, were done for the AGYE2 soil column. The comparison between the AGYE2 records and the estimated site response is shown on Figure 7. For the EW component, there is a good agreement between the estimated and measured spectra for all periods, while in NS, the long-period response from 0.9 to 2.5 s was underestimated by using the 1.2 scaling factor. The PGA at both AGYE2 components matched the estimated site response. The difference in the sedimentary rock lithology at UCSG and the igneous rock at AGYE TP, combined with possible topographic effects due to the intrusion of the igneous rock could have influenced the NS component at AGYE TP station. At AGYE2 station, the Sa for this deep soft site was 10 times higher than UCSG at the site's inelastic site period of 1.65 s.

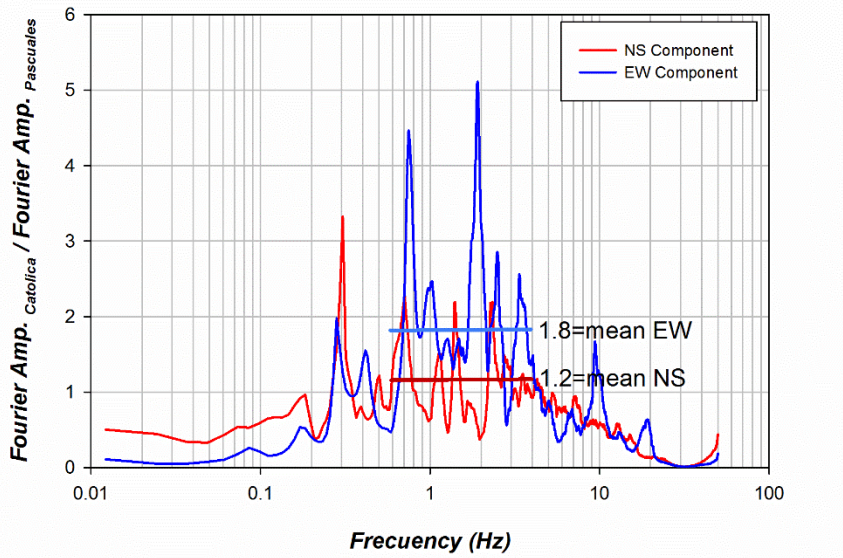

Figure 6. Fourier amplitude spectra ratio between UCSG and AGYE PT stations

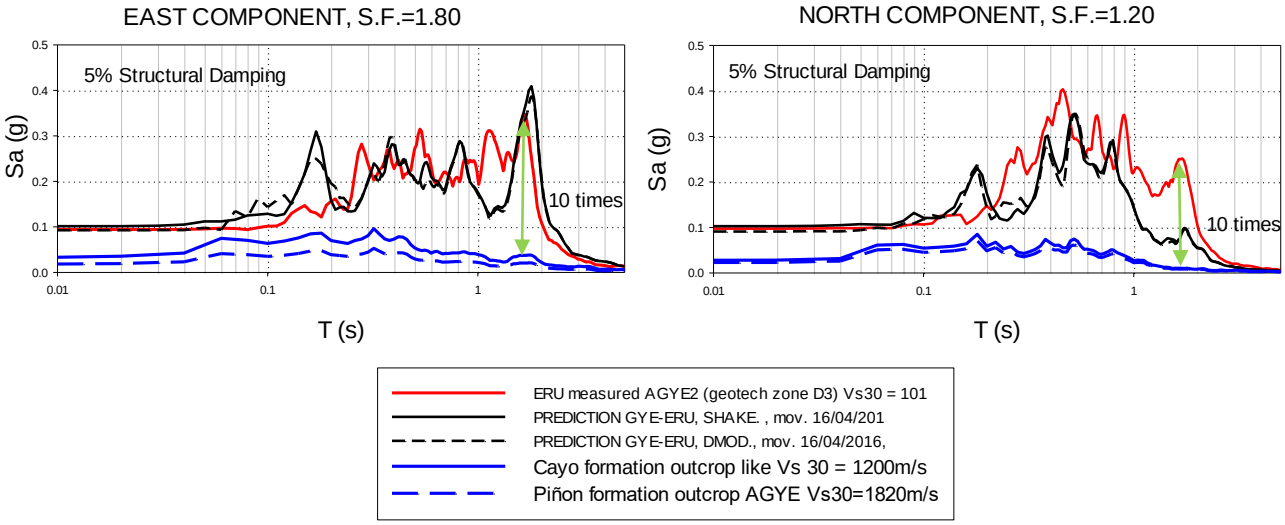

Figure 7. Predicted and measured spectra in AGYE2 station by propagating the scaled AGYE TP record

A deconvolution analysis was performed from the AGYE2 Ramon Unamuno record within Zone D3a with similar response observed in the estimated maximum shear strain, induced G/G_{max} and cyclic stress ratios, CSR

($0.65\tau_{max}/\sigma'_{vo}$) for the EW and NS components by propagating the scaled AGYE TP record in AGYE2 soil column (Figure 8). The levels of accelerations in the 2016 event were similar to the ones in the 1942 event. In the 2016 earthquake the overall behavior was satisfactory with only few structures collapsing, several buildings with structural damage and some buildings with nonstructural damage.

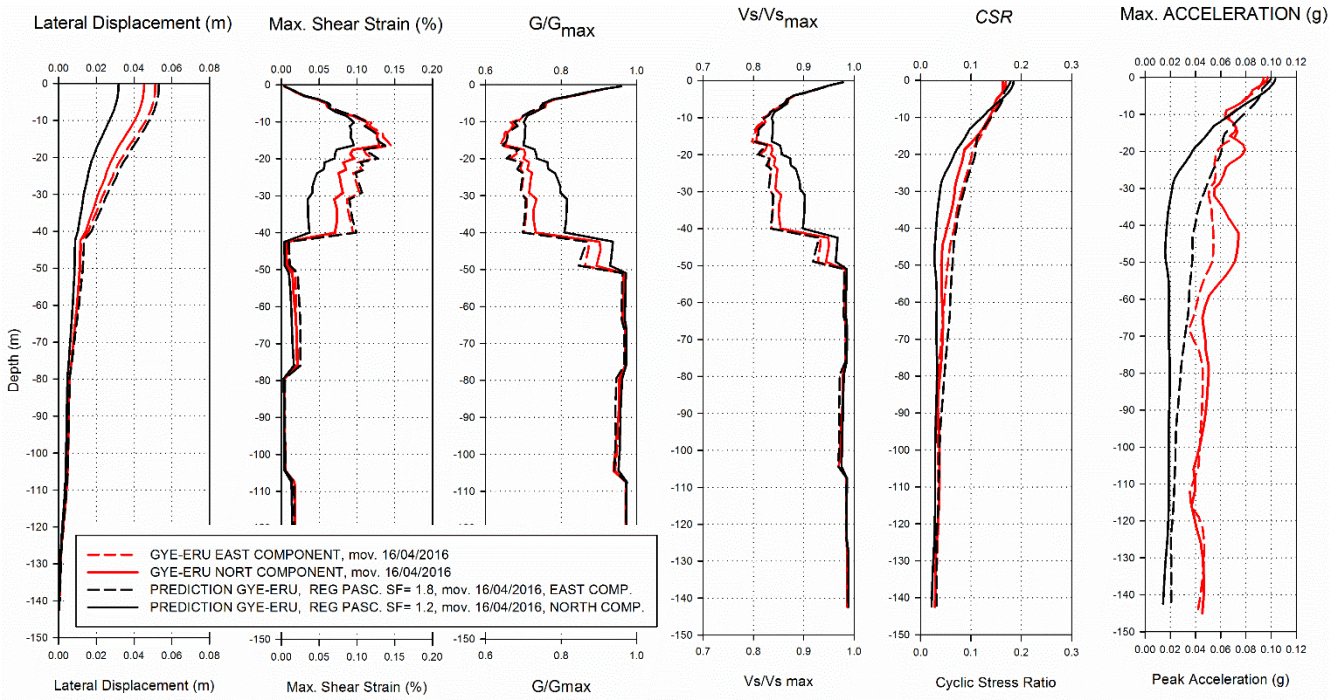

Figure 8. Lateral displacement, max shear strain, G/G_{max} and $V_s/V_{s\ max}$, CSR, and max acceleration comparison between the predictions and measurements at the AGYE2 station.

4. Liquefaction

Liquefaction was observed at the affected coastal areas due to presence of loose granular soils and shallow groundwater, with several cases in the city of Manta and along the Portoviejo River[1, 2]. Two macro-landslides in Manabí were likely triggered by increment in water pressure and loss of soil strength due to possible liquefaction not evident at the surface near the landslides. Evidence of liquefaction with flooding and settlements was detected during the GEER-ATC army helicopter flyover as shown on Figure 9[1] with potential sand ejecta.

Figure 9. Liquefaction evidence from helicopter flyover of Manabí coast from the GEER-ATC reconnaissance mission [1] (GPS, left: 0°39'41.8"S, 80°18'46.6"W; right: 0°12'31.7"S, 80°15'22.5"W)

4.2 Port of Manta

Massive liquefaction damage was observed at Mant, located 76 km from the epicenter, mainly at Tarqui area and the Port. Manta Port consists of two pile supported piers, a rock breakwater and embankment, a piled wharf and four parking lots as shown in Figure 10. Liquefaction and liquefaction-induced phenomena were evident throughout the port, some of the damages caused by liquefaction and lateral spreading were the following. - Cracks parallel to the rock berm in Lot 500 developed. - Soil boils erupted from vents in the pavement. - Foundations for light poles rotated approximately 2º towards the rock berm and sunk into the ground. - A boat ramp on the southeast side of the area with 4-m high reinforced concrete retaining wall moved about 40 cm outward at the top of the wall. Major liquefaction was observed in the car lots of the port, particularly in Lot 500 as is shown in Figure 10. Cracks of over 300 m extended throughout the lot, parallel to the rock berm and a vast amount of sand and silt were ejected as is shown in Figure 11.

Seven SPT tests were performed in Lot 500 as is shown in Figure 11 and the liquefaction potential and volumetric settlements were evaluated by various authors[8] [9] [10] [11] [12] [13] [14] . In adittion, several CPTu tests were performed in the lot area and the liquefaction potential and post-liquefaction effects were evaluated. Figure 11 shows the location of CPTu-2 in the parking lot, while Figure 13 presents the liquefaction potential estimated by the method of Idriss & Boulanger (2008)[12] and Robertson (2009)[9], and the volumetric settlement and lateral displacement estimated by the method of Zhang et al. (2002, 2004) [11] [13] and Idriss & Boulanger (2008)[11]. The method of Idriss and Boulanger (2008) [12] considers the Fines Content variation, thus this was calibrated with a SPT boring performed close to CPTu-2. It can be seen that the method of Zhang et al. (2002, 2004) [11] [13] yields closer predictions to the measured lateral deformations.

A comparison of the estimations and the measurements in each of the SPT locations is shown in Figure 13. It can be observed that Cetin et al. (2009) [8] and Moss et al. (2006) [10] yield closer estimations to the observed in field.

(a) (b)

Figure 10. (a) Elements in Manta Port (Google Earth, 2016) and (b) Sand ejection and cracks in Lot 500 produced by the earthquake. For details see [1]

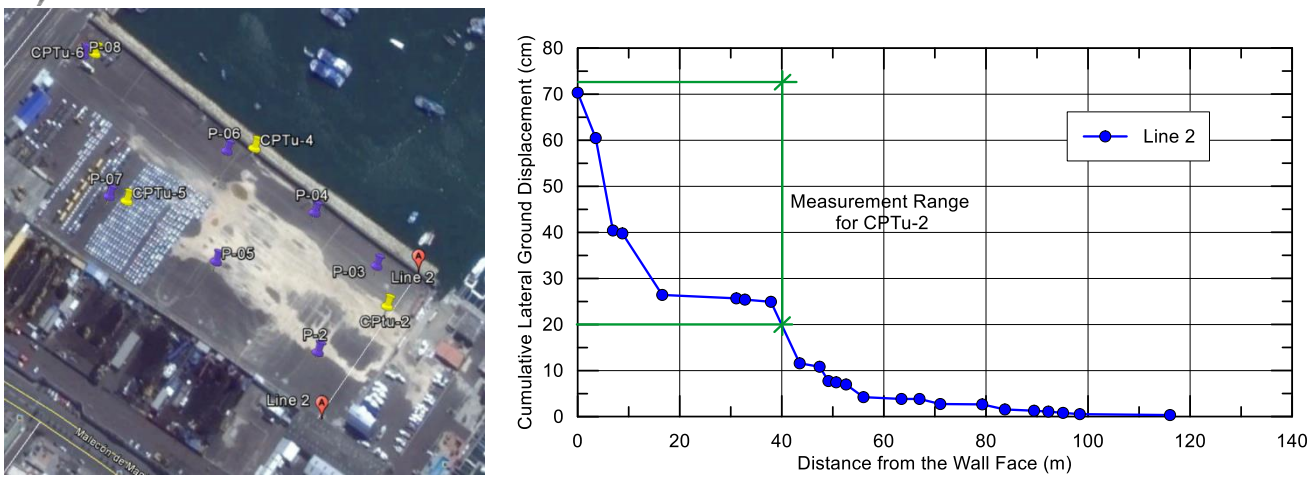

Figure 11. (a) Location of line 2 in Lot 500, (b) Cumulative lateral spread displacements measured along Line 2.

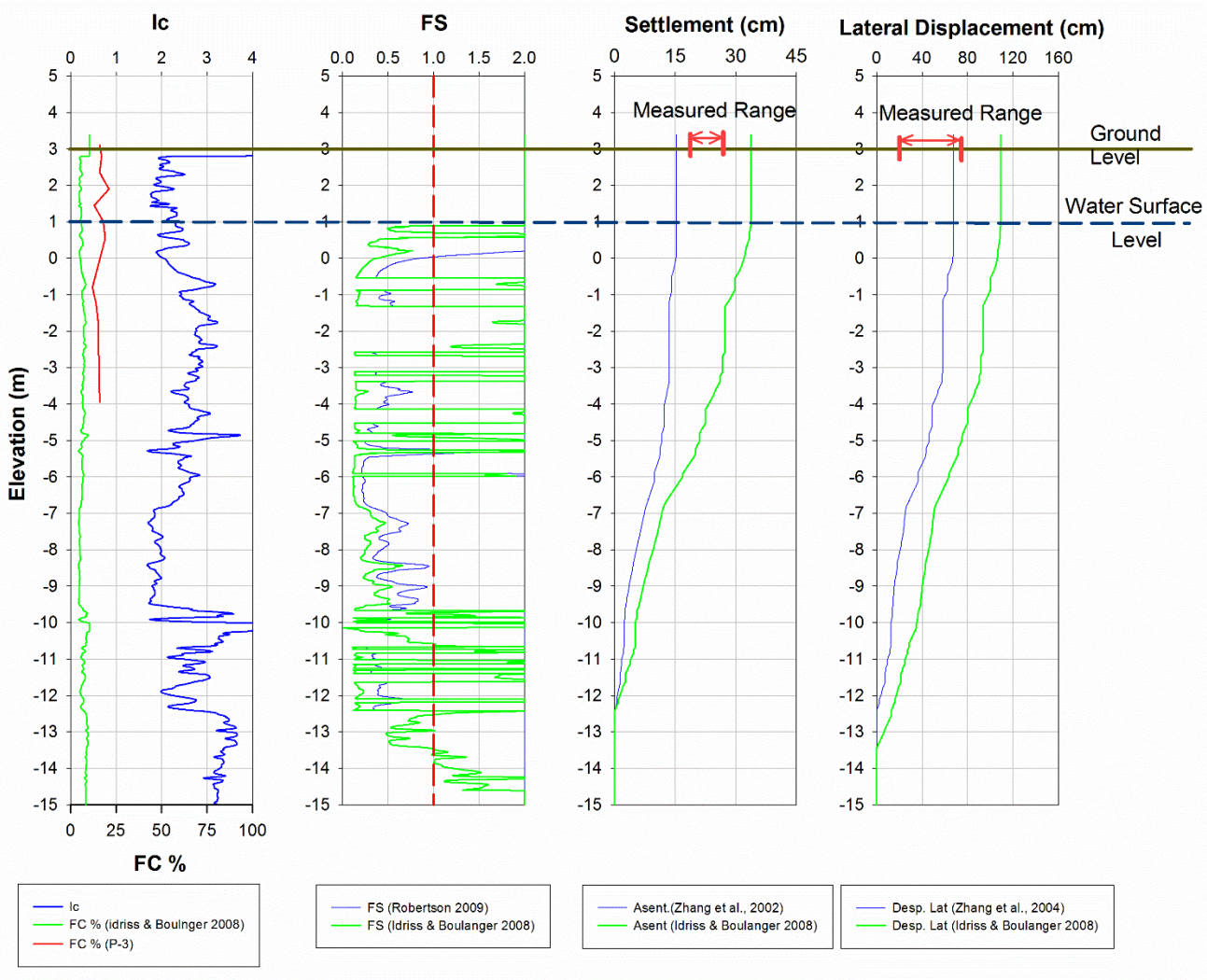

Figure 12. Liquefaction potential and lateral displacement evaluation for CPTu-2 in Lot 500.

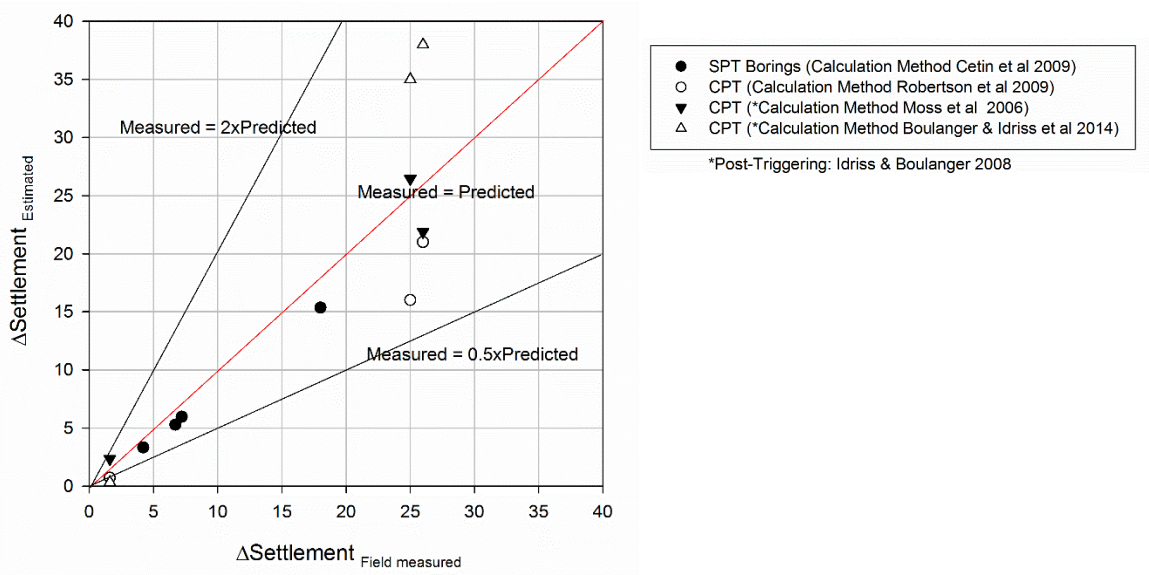

Figure 13. Post-liquefaction volumetric settlement (in cm) calculated and measured at Lot 500 in Manta Port.

4.3 Mejia Embankment

This section presents observations of poor behavior of a bridge approach embankment, whose failure impacted local connectivity, ability to quickly receive supplies, and access of emergency vehicles. The bridge is Mejia Bridge, located about 8 km north of Portoviejo.

The location of a SPT and CPTu tests performed after the earthquake are presented on Figure 14. In addition, an aerial view of the failure at the Mejia Bridge site (by COE-3) is shown Figure 15 with sketched markups of the observed movement of the embankment along assumed failure planes. The failure planes appear to be either along the interface between the embankment and the foundation soils (planar surface) or through the foundation soils. The latter, indicative of a more circular surface failure may be due to liquefaction-induced softening that allowed the reduced-strength soil to shear in the earthquake.

Figure 14. Location of the SPT and CPT tests performed at Mejia Bridge

Figure 15. Mejia Bridge. Right: Aerial view of embankment failure with assumed movement and failure modes marked with yellow (after COE-3, GPS: 0°59'24"S, 80°28'11"W). Left: Embankment view after earthquake. For details see [1].

The south west abutment and gabions of the Mejia Bridge displaced downward and rotated away from the embankment. The north abutment exhibited little damage to the walls and gabion slope adjacent to the bridge, with some settlement and/or rotation of the slope next to the NE wing wall (Figure 16).

The liquefaction potential and post-liquefaction effects were evaluated for the SPT P-01 located at the top of the embankment and the results are presented in Figure 17. For fine grained soils criteria of Bray and Sancio (2006)[15], which is based on the PI and w_c/w_L was considered. Consequently, soils that due to its index properties are not susceptible to liquefaction were not evaluated in post liquefaction analysis. Additionally, it is assumed a similar effect on triggering effects of the fines content on the lateral spreading. The large value of displacement estimated of 1.7 m would indicate the failure in the embankment.

Figure 16**.** Mejia Bridge. Left: Failures of SW abutment and gabions (GPS: 0°59'23.5"S, 80°28'11.6"W). Right: North abutment performance (GPS: 0°59'24.94"S, 80°28'11.26"W). For details see [1].

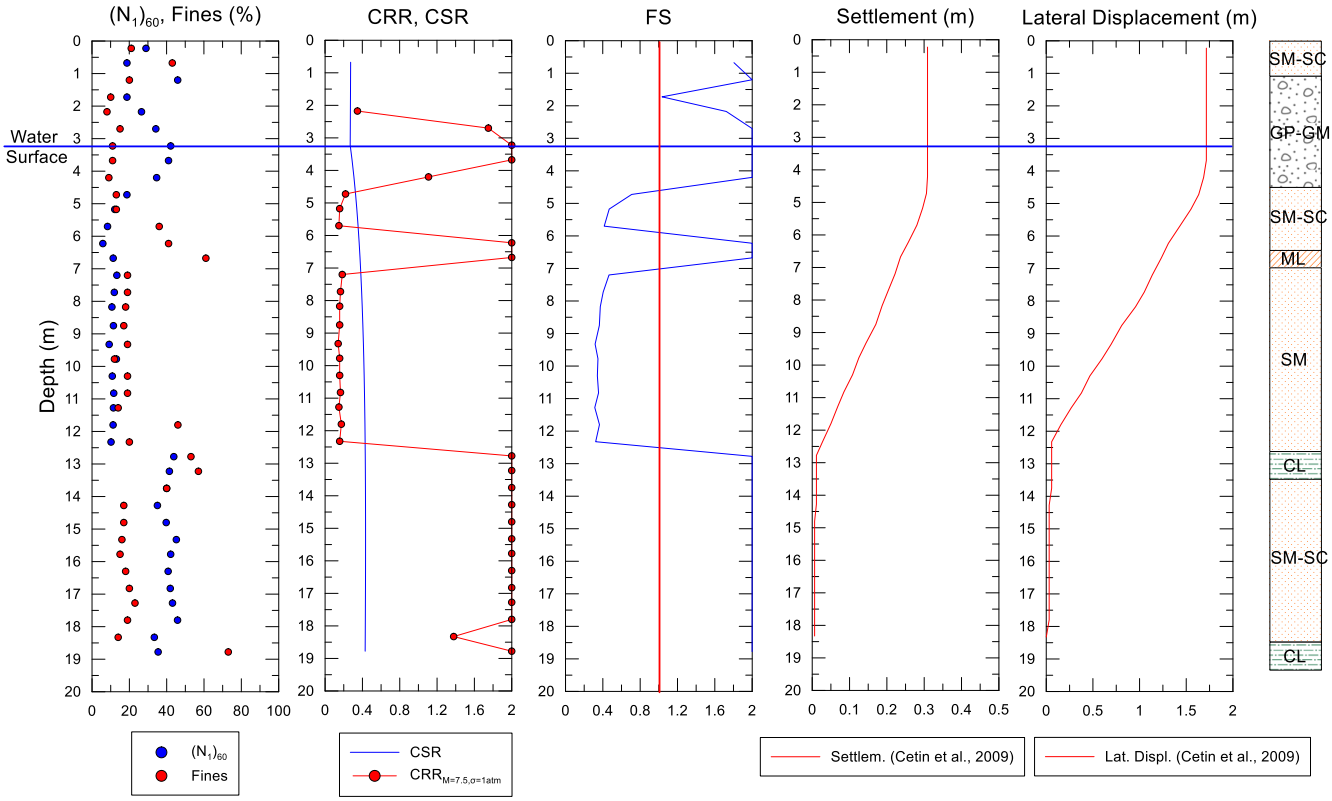

Figure 17. Liquefaction potential and post-liquefaction evaluation for P-01 Mejia Bridge Embankment.

5. Conclusions

As can be seen from the analysis, the 2016 M_w7.8 Muisne earthquake was one of the most damaging earthquakes of this century with devastating impact in Ecuador's built and natural environment, particularly in the province of Manabi, as well as the country's economy. The ground motions were intense and in some cases exceeded design levels. Factors that contributed to the intensity of the motions included the difficult subsurface conditions with potentially liquefiable loose sands. The April 16 event could be considered as a frequent motion for Guayaquil City. Although the source-to-site distances was around 170 km, the deep soft deposits of Guayaquil sediments highly amplify the ground motion resulting in an undesirable building performance; however many cases have shown that some structures behaved in a resilient manner.

6. Acknowledgements

The information contained in this paper is based on the GEER-049 report titled "GEER-ATC Earthquake Reconnaissance: April 16 2016, Muisne, Ecuador." This work was supported by the National Science Foundation through the Geotechnical Engineering Program under Grant No. CMMICMMI-1266418. The Geotechnical Extreme Events Reconnaissance GEER Association is made possible by the vision and support of the NSF Geotechnical Engineering Program Directors: Dr. Richard Fragaszy and the late Dr. Cliff Astill. GEER members donate their time, talent, and resources to collect time-sensitive field observations of the effects of extreme events. Financial contribution from the Applied Technology Council (ATC) funded the participation of two structural engineers in the mission. US agencies, academic institutions, and individuals volunteered with time and/or resources, all gratefully acknowledged in Chapter 3 of [1]. The engineering firms of WSP | Parsons Brinckerhoff (WSP|PB) and Gilsanz, Murray, Steficek, LLP (GMS) provided staff time and resources. Our colleagues in Ecuador were instrumental in providing local assistance and data, for which we are grateful and acknowledge in Chapter 3 of [1]. For this Part 2 paper, we would particularly like to acknowledge the Ministries of Urban Development & Housing (MIDUVI) and of Transportation & Public Works, the National Geophysical

Institute, the 911 Emergency Response Agency, the Army Polytechnic School (ESPE) and the Army Corps of Engineers (ECACE).

7. References

[1] Nikolaou, S., Vera-Grunauer, X., and Gilsanz, R., eds., 2016. GEER-ATC Earthquake Reconnaissance: April 16 2016, Muisne, Ecuador, Geotechnical Extreme Events Reconnaissance Association Report GEER-049, Version 1. Authored by: Alvarado, A., Alzamora, D., Antonaki, N., Arteta, C., Athanasopoulos-Zekkos, A., Bassal, P., Caicedo, A., Casares, B., Davila, D., Diaz, V., Diaz-Fanas, G., Gilsanz, R., González, O., Hernandez, L., Kishida, T., Kokkali, P., López, P., Luque, R., Lyvers, G.M., Maalouf, S., Mezher, J., Miranda, E., Morales, E., Nikolaou, S., O'Rourke, T., Ochoa, I., O'Connor, J.S., Ripalda, F., Rodríguez, L.F., Rollins, K., Stavridis, A., Toulkeridis, T., Vaxevanis, E., Villagrán León, N., Vera-Grunauer, X., Wood, C., Yepes, H., Yepez, Y. Accessible at the GEER website geerassociation.org.

[2] Diaz-Fanas, G., Nikolaou, S., Vera-Grunauer, X., Gilsanz, R., Diaz, V., 2016. Selected Observations from the April 16, 2016 Muisne, Ecuador Earthquake, in 1st International Conference on Natural Hazards & Infrastructure (ICONHIC).

[3] Reynaud, C., Jaillard, E., Lapierre, H., Mamberti, M. and Mascle, G.H. (1999). Oceanic plateau and island arcs of southwestern Ecuador: their place in the geodynamic evolution of northwestern South America.. Tectonophysics 307: 235-254.

[4] Vera Gruanuer, X. (2014). Elaboración del Documento de la Microzonificación Sísmica y Geotécnica de la Ciudad de Guayaquil según la Norma Ecuatoriana de la Construcción NEC 2011. Guayaquil.

[5] Vera-Grunauer, X. (2014). Seismic Response of a Soft, High Plasticity, Diatomaceous Naturally Cemented Clay Deposit. PhD Thesis, Department of Civil and Environmental Engineering, University of California, Berkley.

[6] Ecuadorian Construction Standards 2015 (Norma Ecuatoriana de la Construcción NEC_SE_CM, 2015) Geotechnics and Foundations Chapter

[7] Pestana, J.M. y Salvati, L. (2006) Small strain behavior of granular soils. part 1. model for cemented and uncemented sands and gravels. Journal of Geotechnical and Geoenvironmental Engineering, 132(8), 1071–1081.

[8] Cetin, K., Bilge, H., Wu, J., Kammerer, A., and Seed, R. (2009). "Probabilistic Models for Cyclic Straining of Saturated Clean Sands." J. Geotech. Geoenviron. Eng., 10.1061/(ASCE)1090-0241(2009)135:3(371), 371-386.

[9] Robertson, P.K. (2009). Performance based earthquake design using the CPT. Keynote Lecture, International Conference on Performance-based Design in Earthquake Geotechnical Engineering – from case history to practice. IS-Tokyo, June 2009.

[10] Moss, R. E. S., Seed, R. B., Kayen, R. E., Stewart, J. P., Der Kiureghian, A., and Cetin, K. O. (2006). CPT-based probabilistic and deterministic assessment of in situ seismic soil liquefaction potential, J. Geotechnical and Geoenvironmental Eng., ASCE 132(8)

[11] Zhang, G., Robertson. P.K., Brachman, R., 2002, Estimating Liquefaction Induced Ground Settlements from the CPT, Canadian Geotechnical Journal, 39: pp 1168-1180

[12] Idriss, I. M., and Boulanger, R. W. (2008). Soil liquefaction during earthquakes. Monograph MNO-12, Earthquake Engineering Research Institute, Oakland, CA

[13] Zhang, G., Robertson. P.K., Brachman, R., 2004, Estimating Liquefaction Induced Lateral Displacements using the SPT and CPT, ASCE, Journal of Geotechnical & Geoenvironmental Engineering, Vol. 130, No. 8, 861-871

[14] Boulanger, R. W., and Idriss, I. M. (2014). "CPT and SPT based liquefaction triggering procedures." Report No. UCD/CGM-14/01, Center for Geotechnical Modeling, Department of Civil and Environmental Engineering, University of California, Davis, CA, 134 pp

[15] Bray, J. D., and Sancio, R. B., (2006). Assessment of the liquefaction susceptibility of fine-grained soils, J. Geotechnical and Geoenvironmental Eng., ASCE 132(9), 1165–1177.